

Simulation of Hydrodynamic Ram and Liquid Aeration

Authors:

S.C.McCallum and D.D.Townsend

BAE SYSTEMS

Correspondence:

Stuart McCallum
BAE SYSTEMS
Mathematical Modelling Department
Advanced Technology Centre
FPC 267 PO Box 5, Filton
Bristol, BS34 7QW
UK

Tel: +44 (0) 117-302-8120

Fax: +44 (0) 117-302-8007

e-mail: stuart.mccallum@baesystems.com

Keywords:

Hydrodynamic Ram, High Velocity Impact, Failure, Aeration, Tait EOS

ABSTRACT

During the past several years, research within BAE SYSTEMS has concentrated on developing a capability for simulating Hydrodynamic Ram (HRAM). In this paper we demonstrate how the ALE technique in LS-DYNA can be used to simulate the principal stages of HRAM with liquid aeration.

LS-DYNA is used to simulate the impact of a small steel sphere at 2km/s into a water-filled container manufactured from 3.2 mm thick aluminium alloy L165. The simulation results are compared with laboratory experiments from a two-stage gas-gun facility showing close agreement with peak pressure and impulse values. In additional simulations, aeration is modelled using an effective equation of state, which describes the compressibility of the water (on a macro-scale) inside the container. The simulation results show that aeration can be used to alleviate the shock wave that forms ahead of the projectile in order to reduce damage on the surrounding structure.

INTRODUCTION

Hydrodynamic Ram (HRAM) occurs when a high-velocity projectile penetrates a fluid-filled container and transfers its momentum and kinetic energy through the fluid to the surrounding structure. In most circumstances the term HRAM is associated with the result of excessive structural damage during the transfer of the projectile energy. HRAM is of particular concern in the design of wing fuel tanks for aircraft and may also be observed for land, sea and space vehicles from e.g. uncontained engine debris, tyre rubber or orbital debris impact [1], [2].

There are five principal stages of HRAM referred to as penetration, shock, drag, cavitation and exit. In each stage there are complex interactions between the projectile, fluid and container. The penetration stage results from the initial impact of the projectile with the container wall and fluid. This stage is followed by the formation of a high-pressure hemispherical shock front that propagates ahead of the projectile. The shock front interacts with walls of the container and may produce outward petaling of the entrance panel. As the projectile translates through the container it begins to transfer a quantity of its momentum to the fluid. This drag stage causes the projectile to decelerate and results in the formation of a cavity within the wake region of the projectile. The final stage of HRAM occurs when the projectile exits the container. In contrast to the penetration stage, the exit of the projectile occurs through a pre-stressed wall, caused by the initial shock stage and subsequent loading by the fluid.

The work presented in this paper demonstrates how the ALE technique in LS-DYNA can be used to simulate HRAM. LS-DYNA is used to simulate the impact of a small steel sphere at 2km/s into a water-filled container manufactured from 3.2 mm thick aluminium alloy L165. The simulation results will be compared with laboratory experiments from a two-stage gas-gun facility for validation of peak pressure and impulse values within the water.

In additional simulations, an aeration model is implemented which increases the compressibility of the water inside the container; experiments have shown that shock-wave pressure and velocity can be reduced by adding gas bubbles to water (aeration). The aeration model is presented as an equation of state, which describes the effective compressibility of the mixture (on a macro-scale) inside the container for three volume fractions of air (1%, 5% and 10%). Simulation

results using the aeration model are presented to demonstrate the effectiveness of this technique for reducing shock-wave strength.

Methodology

The HRAM simulations presented in this section are performed using the ALE technique within LS-DYNA 970 [3]. The computational domain is defined in quarter symmetry and consists of 4 principal parts: projectile, container, water and air (void) shown in Figure 1. The projectile and container walls are modelled using Lagrangian elements, while the water and void regions are represented by Eulerian elements. The void region is included to allow movement of the water during displacement and failure of the container walls. The Lagrangian and Eulerian parts are coupled using the `*CONSTRAINED_LAGRANGE_IN_SOLID` keyword [3].

The Lagrangian mesh was constructed from 3500 shells (container); 84000 hexahedral Eulerian elements were used to define the water and void. The modelling approach used in these simulations will demonstrate the accuracy of LS-DYNA for predicting the water pressure and impulse during HRAM.

Model Construction

The model geometry and computational mesh for each each part was generated using the pre-processing software HyperMesh [4]. Mesh sensitivity studies were performed in earlier work to determine the convergence behaviour (pressure) of the simulation results for varying mesh size. Details of the material models and parameters used in each part are given in the following sections.

Material Models

Projectile

The projectile is modelled using solid hexahedral elements with element formulation 1 – constant stress solid element. The material is defined as a rigid body using material type 20 using material parameters representative of S-7 tool steel [5]: $\rho = 8.157 \text{ g/cm}^3$, $E = 2.0 \text{ Mbar}$ and $\nu = 0.3$. The Young's modulus and Poisson's ratio are defined to allow calculation of the sliding interface parameters used during contact analysis.

Walls

The walls of the rectangular container are modelled using Lagrangian shell elements with element formulation 2 – Belytschko-Tsay and a thickness of 3.2mm. The material is defined by material type 24 – piecewise linear plasticity using material parameters representative of L165/L167 also known as 2014A-T6: $\rho = 2.77 \text{ g/cm}^3$, $E = 0.71 \text{ Mbar}$, $\nu = 0.3$, $\sigma_y = 3.26\text{E-}03 \text{ Mbar}$, $E_{TAN} = 7.1\text{E-}03 \text{ Mbar}$. The yield strength was increased by a factor of 3.5 to account for strain-rate effects. The failure of the material is controlled by a plastic strain to failure criteria $\epsilon_{fail} = 0.22$. If this failure value is exceeded during the simulation the associated element is deleted from the analysis.

Water

The water is modelled using solid hexahedral elements with element formulation 12 – 1 point integration with single material and void. The non-aerated water is defined using the null material type 9 in combination with a Grüneisen equation of state form 4 [3]. A linear relationship between the particle velocity u_p and shock velocity u_s was assumed, i.e. $u_s = c_0 + s u_p$. The material parameters, $c_0 = 1.4829 \text{ km/s}$ and $s = 2.0367$ were obtained from published data [6].

The null material type is also used in simulations with aeration, however in this case the density is modified to account for the presence of the air. The Grüneisen equation of state is then replaced with a tabulated equation of state using equation of state form 9. The tabulated equation of state model is linear in internal energy and relates the volumetric strain ε_v (natural logarithm of the relative volume) to the pressure through the parameter C. The parameters used in the aerated equation of state are obtained using the procedure presented in the results section.

Air - Void

The presence of the air outside of the container is also modelled using solid hexahedral elements, however their position is localised around the area of projectile penetration (entry and exit walls). In order to increase the speed of the solution process the material is defined using null material type 9 combined with the keyword **INITIAL_VOID* [3]. In this case the elements are approximated as fluid elements with very low densities.

Experiments

The experiments were conducted at BAE Systems (Advanced Technology Centre - Impact Facility, Filton, UK). The projectiles used in the experiments were accelerated to the required velocity using a two-stage gas gun (helium driven). The projectile velocity was measured using a series of magnetic velocimeters placed in front of the target container. Imacon and Ultra 68 high-speed cameras were then used to observe the shock wave and projectile motion within the fluid. Shock wave pressure and velocity measurements were recorded using tourmaline transducers and quartz crystal sensors positioned within the tank. The pressure transducers were located in the positions shown in Figure 2. The residual velocity of the projectile on exiting from the tank has been determined using make-screens. Using high-speed photography detailed observations have been made of the HRAM process combined with comprehensive shock pressure measurement.

Simulation Results

HRAM Simulation

As the projectile impacts the front wall a hole is formed which is of similar size and shape to the original projectile. The projectile then translates through the water in the direction of impact, forming a cavity (void region), Figure 3a. During this stage a hemispherical pressure wave (shock front) is formed ahead of the projectile, Figure 3b. This pressure wave reaches a peak magnitude immediately after impact then reduces in strength as the projectile translates through the water. The projectile continues to decelerate through the water before penetrating the rear wall.

In order to assess the accuracy of the HRAM model, simulation results for pressure are compared with the experiment results at six locations within the container, Figure 4. This comparison shows good general agreement for peak pressure and impulse. The simulation results are most accurate for positions close to the impact point and near to the trajectory path (transducer A, B and D). However, pressure predictions for positions close to the exit wall (transducer E and F) did not capture the reflected wave, which is evident as a sharp spike in the experiment results. It should be possible to simulate this reflecting wave using a finer mesh resolution in the water.

Aeration Model

In the previous simulation we modelled the liquid within the container as an incompressible material (water). However, experiments suggest that shock-wave strength can be reduced by increasing the compressibility of the liquid [7]. This can be achieved by aerating the liquid with small gas bubbles. In practice, the liquid would only need to be aerated when a threat is present allowing the container volume to be maximised for fuel during flight.

The interaction of a shock wave with a gas bubble is complicated since it can cause bubble collapse, resulting in a jet formation and shock reflections. It is not practical to resolve this level of detail on the scale of an aircraft fuel tank (single shock-bubble simulations are computationally intensive). However, we can use an equation of state to account for the additionally compressibility of the aerated liquid. Although this approach does not model the effects of bubble collapse it does provide a description of the mixture's bulk behaviour. A simple aeration model is developed by combining the Tait EOS for water with the ideal gas law for air. The Tait EOS for water is given by:

$$c = \sqrt{\frac{\gamma(p+B)}{\rho}}, \quad (1)$$

where c is the wave speed, p is pressure, ρ is density and γ and B are measured coefficients. The ideal gas law for air is given by:

$$c = \sqrt{\frac{\gamma p}{\rho}}, \quad (2)$$

where γ represents the ratio of specific heats.

Equations 1 and 2 are then combined to give the effective compressibility of the mixture:

$$\bar{\kappa} = \phi_w \kappa_w + (1 - \phi_w) \kappa_a, \quad (3)$$

where ϕ is the volume fraction and subscripts w and a denote water and air respectively. The compressibility of water is given by:

$$\kappa_w = 1/\gamma_w(p+B), \quad (4)$$

where $\gamma_w = 7.31$ and $B = 3.0E+08$ Pa. The compressibility of the air is written as:

$$\kappa_a = 1/\gamma_a p, \quad (5)$$

where $\gamma_a = 1.4$

If we assume the water is aerated with an even distribution of small gas bubbles the pressure-volumetric strain relationship for the mixture as ϕ tends to 1 can be determined by solving the following steps:

1. Increment volumetric strain

-
2. Calculate effective compressibility of mixture
 3. Calculate increase in pressure
 4. Calculate the volumetric compression of the liquid and gas phase
 5. Calculate new volume fraction of water

An example plot of pressure as a function of volumetric strain is shown in Figure 5 for pure water and air volume fractions of 1%, 5% and 10%. When pure water is aerated at a constant air volume fraction, the compressibility of the mixture is shown to increase, i.e. less pressure is required to obtain the same volumetric strain when compared with pure water, Figure 5. However, when the pressure is increased the volume fraction of gas is reduced; as a consequence the overall compressibility of the mixture is reduced. The compression of the gas phase is evident by the small gradient where the pressure is low. When the gas volume fraction is close to zero the pressure increases rapidly indicating low compressibility.

Aeration during HRAM

The effectiveness with which aeration reduces the shock pressure during HRAM is shown by comparing simulation results for pure water and water with air (volume fraction of 10%), Figure 6. In the pure water case the incompressibility of the water results in a strong pressure wave that propagates rapidly through the liquid. However, when aeration is applied the magnitude of the pressure front and the propagation speed are both reduced. The effects of aeration are demonstrated further by comparing plastic strain of the rear wall. In the pure water case a hole is formed at the centre of the rear wall that propagates vertically forming a tear near to the container edges, Figure 7a. The simulation results for aeration predict similar plastic strain around the impact area; however, the extent of the vertical tearing is reduced significantly, Figure 7b.

Summary and Conclusions

Hydrodynamic Ram (HRAM) occurs when a high-velocity projectile penetrates a fluid-filled container and transfers its momentum and kinetic energy through the fluid to the surrounding structure. It is an event that can cause extensive structural damage during the transfer of the projectile energy.

In this paper, simulation results are presented using a modelling methodology to accurately predict the principal stages of HRAM. The ALE technique was used to simulate the impact of a small steel sphere at 2km/s into a water-filled container manufactured from 3.2 mm thick aluminium alloy L165. The simulation results were compared with experiments showing close agreement to peak pressure and impulse within the water.

In additional simulations, an aeration model was implemented to increase the compressibility of the water inside the container. The simulation results show a reduction in shock-wave pressure and structural damage with increasing compressibility.

Acknowledgements

Thank you to Dr N. Park and Dr P. Deval from BAE SYSTEMS (Filton, UK) for providing the experiment results. Thank you also to Mr C. Constantinou from BAE SYSTEMS (Filton, UK) for guidance on HRAM modelling.

References

- [1] Mousa NA, Whale MD, Groszmann DE, and Zhang XJ. The potential for fuel tank fire and hydrodynamic ram from uncontained aircraft engine debris. U.S. Department of Transportation, Federal Aviation Administration. Washington, D.C. 20591 DOT/FAA/AR-96/95, 1997.
- [2] Anderson J, Charles E., Sharron TR, D. Walker J, and Freitas CJ. Simulation and analysis of a 23-mm HEI projectile hydrodynamic ram experiment. International Journal of Impact Engineering 1999; 22, (9-10):981-997.
- [3] LS-DYNA - Keyword User's Manual Version 970: Livermore Software Technology Corporation, April 2003.
- [4] HyperMesh revision 5.1. Altair Computing, Inc., Altair Engineering Ltd, Vanguard Centre, Sir William Lyons Road, Coventry, CV4 7EZ, 2003.
- [5] Johnson GR, and Cook WH. A constitutive model and data for metals subjected to large strains, high strain rates and high temperatures, Proceedings of the 7th International Symposium on Ballistics. The Hague (Netherlands), 1983. pp. 541-547.
- [6] van Thiel M. Compendium of shock wave data, UCRL-50108, Vol. 2, Rev. 1 ed: Lawrence Livermore Laboratory, 1997.
- [7] Burt PL. Advance report on the ballistic shock absorption test. part 2: fluid aeration. British Aerospace Defence. Issue 1, BAE-WSD-AR-RES-ARM-000209, 1995.

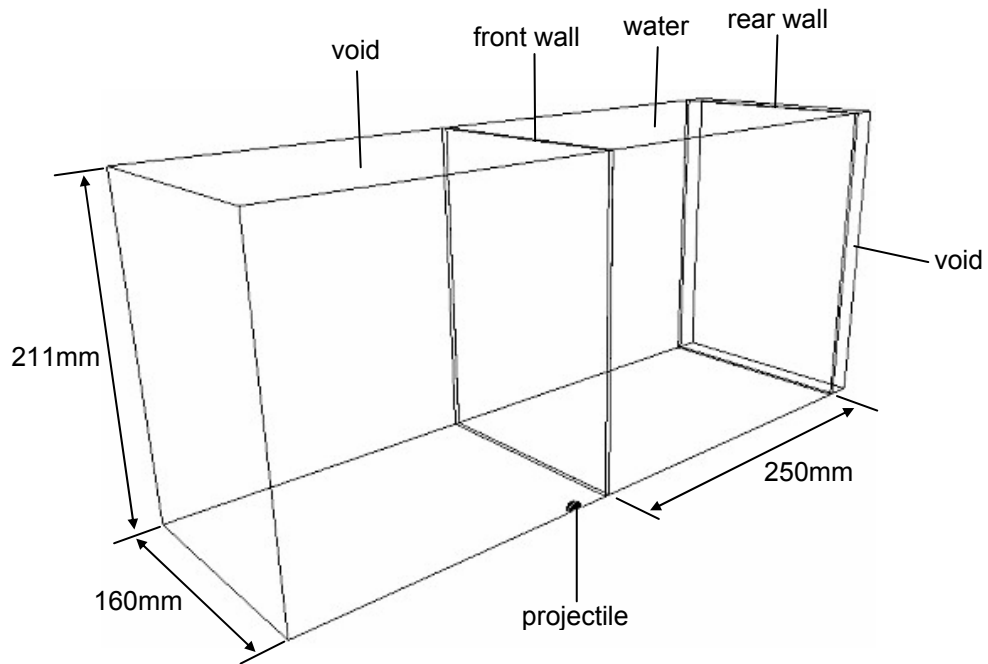


Figure 1 Schematic showing the computational domain of the HRAM model – $\frac{1}{4}$ symmetry.

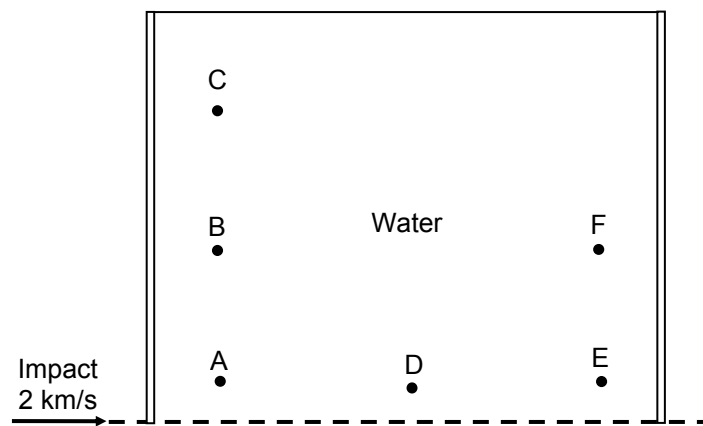


Figure 2 Schematic showing the pressure measurement positions (A-F) inside the rectangular container – $\frac{1}{4}$ symmetry.

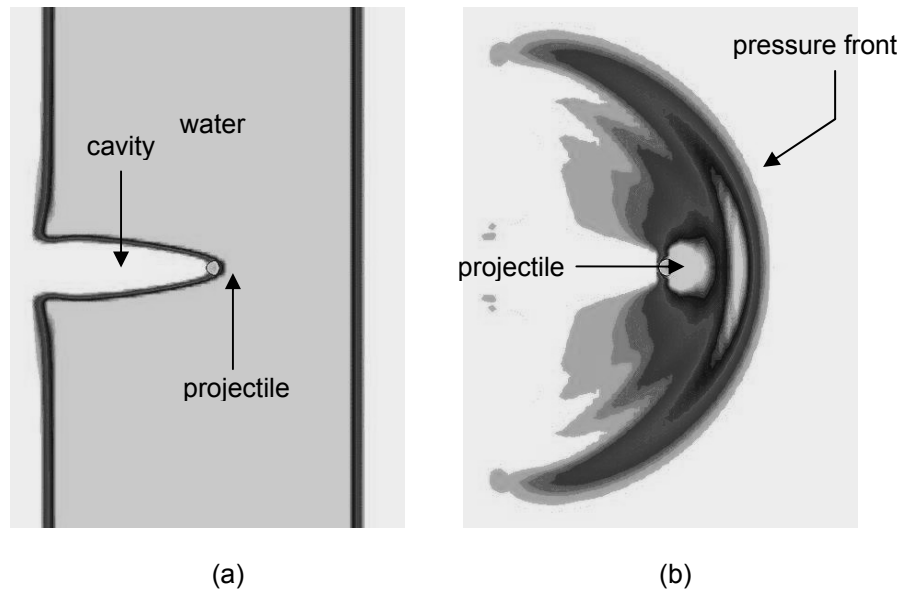
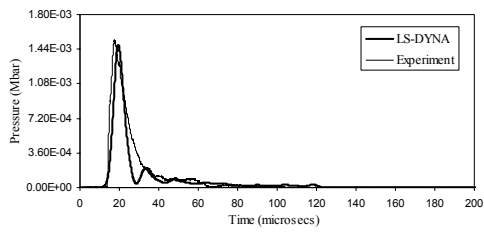
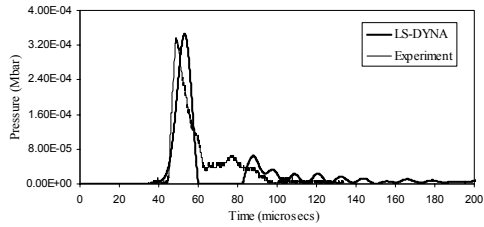


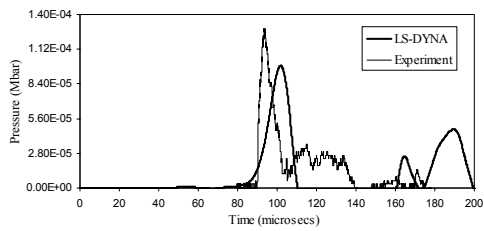
Figure 3 Simulations results showing (a) cavity formation and (b) hemi-spherical shock front during translation of the projectile through the water.



Position A

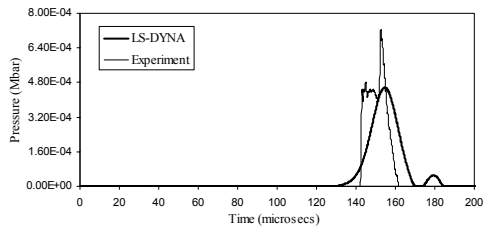
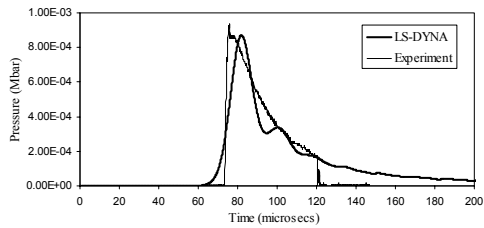


Position B



Position C

Position D



Position E

Position F

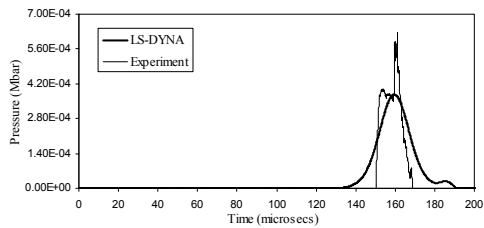


Figure 4 A comparison of simulation and experiment results for pressure (water) at six different positions (A-F) inside the container.

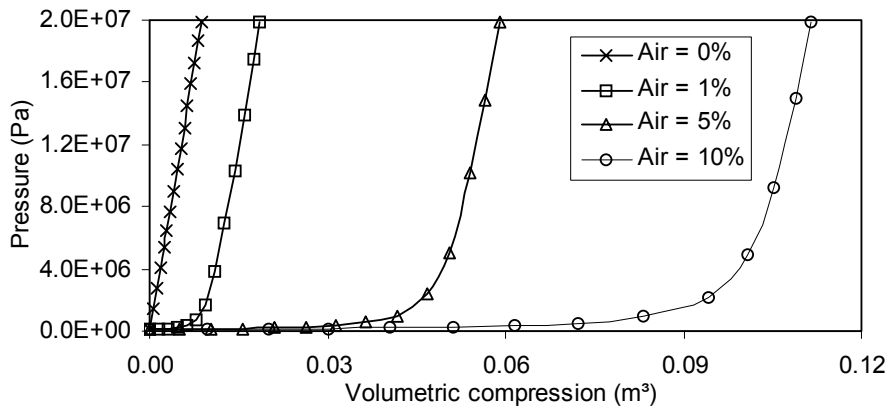


Figure 5 Pressure – volume relationship, comparing the compressibility of water with aerated water for three aeration levels (1%, 5% and 10%).

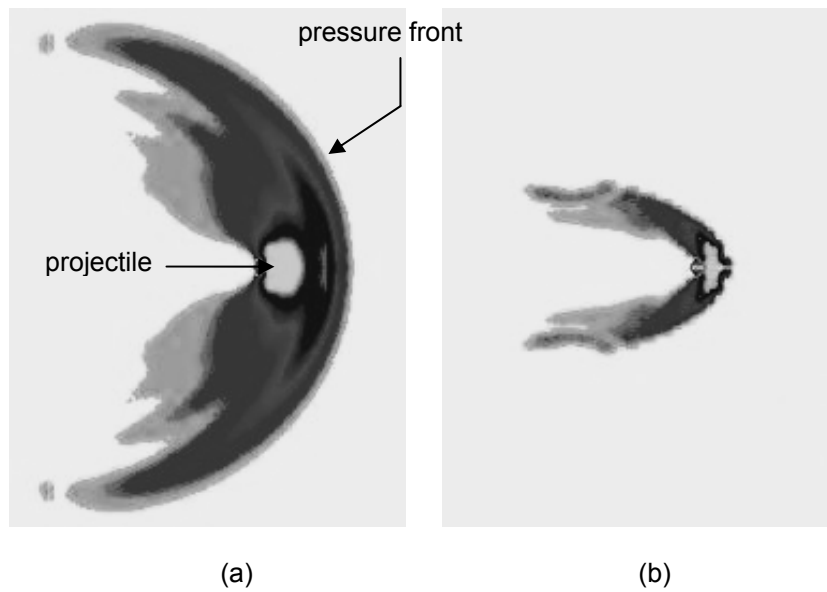


Figure 6 Simulation results showing the shock front ahead of a non-spherical projectile in (a) water and (b) water with 10% aeration.

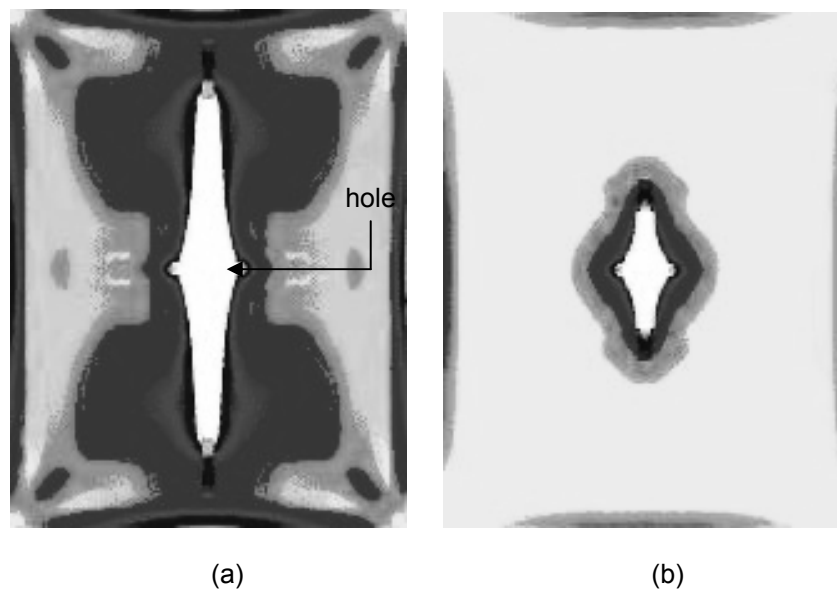


Figure 7 Simulation results showing damage caused to the exit wall of a container filled with (a) water and (b) water with 10% aeration.